

## Effect of $\text{SiO}_2/\text{Al}_2\text{O}_3$ ratio on the whiteness of ceramic tile engobes with low zircon content

S. Ö. Varışlı<sup>1,2\*</sup>, F. Taşkıran<sup>1,3</sup>, B. Öztürk<sup>1,4</sup>, B. Çiçek<sup>2</sup>

<sup>1</sup>Akcoat Advanced Chemical Coating, Materials Research and Development Center,

<sup>2</sup>nd Organized Industrial Zone, 54300 Hendek, Sakarya, Türkiye

<sup>3</sup>Yıldız Technical University, Department of Metallurgical and Materials Engineering, Istanbul, Türkiye

<sup>4</sup>Yıldız Technical University, Department of Chemical Engineering, Istanbul, Türkiye

<sup>4</sup>Sakarya University of Applied Sciences, Department of Metallurgical and Materials Engineering, Sakarya, Türkiye

### Abstract

Micronized zircon ( $\text{ZrSiO}_4$ ) is used as an opacifier in the production of engobes, opaque glazes, and floor tile bodies. Elevated price levels incentivize researchers to develop alternative engobe formulations with reduced zircon ratios. In this study, new engobes with low zircon content were developed with varying  $\text{SiO}_2\text{-Al}_2\text{O}_3$  mixtures. The effect of the  $\text{SiO}_2/\text{Al}_2\text{O}_3$  ratio on the performance and opacity of the wall and floor tile engobes was investigated. It has been observed that the amount of zircon in the sample compositions could be reduced up to 40% by optimizing the refractoriness-water absorption balance of the engobe with the  $\text{SiO}_2/\text{Al}_2\text{O}_3$  ratio while keeping the opacity in the preferred levels. The color difference ( $\Delta E$ ) value relative to the standard surface was below 1, which is acceptable for visual perception for all the samples. Other measurements such as water absorption and firing shrinkage of the floor tile samples were found to be compatible with the standard composition.

**Keywords:** ceramic, engobe, opacifier,  $\text{SiO}_2/\text{Al}_2\text{O}_3$  ratio, tile, zircon.

### INTRODUCTION

Ceramic tile covering materials are used in various application areas such as interior and exterior claddings of buildings, floor coverings, and swimming pools [1]. The task of the glaze applied to ceramic products is to protect the product surface from abrasive chemicals, ensure easy cleaning, and prevent water permeability. In addition, they add aesthetic values to the products, which are an important element of the marketing and sales strategies of the manufacturers today [2]. Floor tiles are characterized by having almost zero open porosity and low water absorption (0.5-3%), usually produced with fast firing cycles of 35-60 min at 1180-1250 °C [3-6]. Wall tiles are fired in double fast firing cycles (<45 min) at temperatures between 1080 and 1150 °C [7, 8]. The microstructure and phase composition of a wall tile body are very different and the glassy phase content is less than floor tile body [9]. Due to high water absorption (>10%), they are not suitable for exterior applications. After tiling, the wall tile absorbs water. This absorbed water might appear as traces of water on the tile surface called watermark if the engobe layer is permeable and this is one of the biggest problems for tile manufacturers [10, 11].

Ceramic bodies require the application of an engobe layer, which plays a crucial role in the ceramic tile manufacturing process. The engobe acts as an inert intermediate layer, typically ranging from 100 to 300  $\mu\text{m}$

in thickness, positioned between the glaze layer and the ceramic body [12]. Engobe is used to prevent problems such as cracking and peeling by providing a balance of shrinkage and thermal expansion during firing between the tile body and the glaze [13, 14]. The water permeability of ceramic tiles is primarily attributed to the presence of porosities. The engobe layer serves the purpose of filling these pores, creating a waterproof barrier on the surface of the ceramic tile. By increasing the thickness of the engobe layer, the amount of porosity is reduced, leading to the elimination of watermarks on the tile surface. Furthermore, this increase in engobe thickness enhances opacity, improving the overall appearance of the tile [3-15]. The engobe layer acts as a barrier to water transfer from the wall tile body and color change in the finished product [16]. The production of engobe coatings for ceramic tiles is a rather complex process and largely depends on the choice of raw materials for the composition of the engobe. The main determining factors for raw materials are availability and relatively affordable cost for multi-tonnage production [17]. Traditionally, the basic raw materials used in the production of engobe coatings are clay, kaolin, quartz, and feldspar [18]. Additionally, engobe is a composition with its opacity feature that is applied as the first layer on ceramic tile and covers the color of the body. Engobe opacity mainly depends on these three parameters: the thickness of the layer, the opacity of the solid phase, and the presence of open pores [19]. Opacity is the result of the difference in refractive index between the crystals and the glassy matrix structure [20]. For high refraction, the crystals should not dissolve in the glassy matrix structure with the increase in temperature. Zirconium silicate (zircon)

\* <https://orcid.org/0000-0002-2643-6828>

is the most widely used opacifier with a refractive index value of 1.94. Zircon is widely preferred in the ceramic industry due to its exceptional technical properties. Its high refractive index ( $n$ ) enables it to impart opacity to ceramic tiles, enhancing their visual appearance. Additionally, zircon offers the advantage of improving the chemical and surface abrasion resistance of ceramic tiles. These properties make zircon a valuable material in the production of high-quality ceramic tiles [21]. Besides zircon, mullite ( $n=1.64$ ), alumina ( $n=1.77$ ), quartz ( $n=1.54$ ), akermanite ( $n=1.64$ ) and anorthite ( $n=1.58$ ) are also crystal particles used as opacifiers [22-25]. Zircon and alumina are used to whiten tile bodies and engobes [3-26]. Using alumina instead of zircon increases the opacity and the refractoriness of engobes, therefore causing an increase in their water absorption. By increasing the firing temperature, both the water absorption and the opacity value of the engobe decrease [27]. An alternative way to improve this issue of glazes is to adjust the  $\text{SiO}_2/\text{Al}_2\text{O}_3$  ratio, which determines the amount of crystalline phase that causes the increase in the opacity value [28].

The aim of this study is to reduce the amount of zircon by adjusting the  $\text{SiO}_2/\text{Al}_2\text{O}_3$  ratio of new engobe formulations and to examine the color, water absorption, and firing shrinkage values of the developed samples. For this purpose, different engobe compositions were prepared depending on the variation of  $\text{SiO}_2/\text{Al}_2\text{O}_3$  ratio. In the ceramics industry, the consumption of zircon is significantly higher compared to other industries. Although there is a gradual increase in zircon consumption, its production capacity is unable to keep up with the rising demand. Moreover, the global zircon resources are gradually depleting, leading to a scarcity in supply. Consequently, the limited availability of zircon resources results in increased prices for this material [29].

## EXPERIMENTAL

Industrial grade kaolin (Kaolin, Bulgaria), clay (Etiler, Türkiye), and Na-feldspar (Straton, Türkiye), high purity alpha alumina (99%, 150  $\mu\text{m}$ , Eti, Türkiye), quartz (150  $\mu\text{m}$ , Pomza, Türkiye), zircon (5  $\mu\text{m}$ , Eggerding, Netherland), two commercial opaque frits (containing zircon and titanium dioxide) and a flux frit (Akcoat, Türkiye) were used to produce engobe. The engobe composition in accordance with EN ISO 10545-3 (water absorption determination), EN ISO 10545-8 (linear thermal expansion determination), and EN ISO 10545-2 (dimension and surface smoothness determination) standards was determined and accepted as reference [30-32]. Seger oxide mole contents of floor tile engobe formulations with varying  $\text{SiO}_2/\text{Al}_2\text{O}_3$  ratios are given in Table I. The amount of zircon in the compositions was decreased, and the mole ratio of  $\text{SiO}_2/\text{Al}_2\text{O}_3$  was changed; the weight percentages of some raw materials used in floor and wall tiles are provided in Tables II and III, respectively. Table IV shows Seger oxide mole contents of wall tile engobe formulations with varying  $\text{SiO}_2/\text{Al}_2\text{O}_3$  ratios as well. Table V shows the oxide contents of the raw materials used in the engobe recipes.

Table I - Seger oxide mole contents for floor tile engobe compositions.

Oxide	F-STD	F1	F2	F3	F4
$\text{SiO}_2$	9.48	9.59	9.53	9.48	9.57
$\text{Al}_2\text{O}_3$	1.15	1.18	1.21	1.24	1.21
$\text{K}_2\text{O}$	0.04	0.04	0.04	0.04	0.04
$\text{Na}_2\text{O}$	0.55	0.55	0.55	0.55	0.55
$\text{CaO}$	0.35	0.35	0.35	0.35	0.35
$\text{MgO}$	0.05	0.05	0.05	0.05	0.05
$\text{B}_2\text{O}_3$	0.10	0.10	0.10	0.10	0.10
$\text{ZrO}_2$	0.53	0.46	0.46	0.46	0.44
$\text{SiO}_2/\text{Al}_2\text{O}_3$	8.28	8.15	7.88	7.62	7.92

Table II - Contents (wt%) of some raw materials for floor tile engobe compositions.

Raw material	F-STD	F1	F2	F3	F4
Total zircon	8.0	4.8	4.8	4.8	4.0
Total free $\text{SiO}_2$	36.0	38.4	37.6	36.8	38.4

Table III - Contents (wt%) of some raw materials for wall tile engobe compositions.

Raw material	W-STD	W1	W2	W3	W4
Total zircon	12.0	7.2	7.2	7.2	6.0
Total free $\text{SiO}_2$	10.0	13.6	12.4	11.2	13.6

Table IV - Seger oxide mole contents for wall tile engobe compositions.

Oxide	W-STD	W1	W2	W3	W4
$\text{SiO}_2$	5.21	5.31	5.26	5.20	5.29
$\text{Al}_2\text{O}_3$	0.66	0.69	0.72	0.76	0.72
$\text{K}_2\text{O}$	0.04	0.04	0.04	0.04	0.04
$\text{Na}_2\text{O}$	0.28	0.28	0.28	0.28	0.28
$\text{CaO}$	0.63	0.63	0.63	0.63	0.63
$\text{MgO}$	0.05	0.05	0.05	0.05	0.05
$\text{B}_2\text{O}_3$	0.06	0.06	0.06	0.06	0.06
$\text{TiO}_2$	0.31	0.31	0.31	0.31	0.31
$\text{ZrO}_2$	0.36	0.29	0.29	0.29	0.28
$\text{SiO}_2/\text{Al}_2\text{O}_3$	7.85	7.67	7.25	6.88	7.32

Ten different engobe compositions, consisting of five wall tile engobes and five floor tile engobes, were batched and placed in a porcelain jar containing alumina balls. The mixture was wet-milled for 30 min. Engobe slurries were milled until a sieve residue of 45  $\mu\text{m}$  was achieved between 0-1% for good sinterability [33]. The density of

Table V - Oxide contents (wt%) for raw materials.

Raw material	SiO <sub>2</sub>	Al <sub>2</sub> O <sub>3</sub>	CaO	MgO	ZrO <sub>2</sub>	K <sub>2</sub> O	Na <sub>2</sub> O	TiO <sub>2</sub>	LOI
Kaolin	52.4	32.6	0.15	0.22	-	1.09	0.22	0.19	13.2
Clay	51.8	26.6	0.27	-	-	1.49	0.15	1.17	18.4
Na-feldspar	70.3	17.5	0.88	-	-	-	10.9	-	0.41
Zircon	34.7	2.48	-	-	62.6	-	0.24	-	-
Quartz	99.3	0.42	0.12	-	-	-	-	-	0.14
Alumina	0.07	99.2	-	-	-	-	0.64	-	0.06

the slurries was adjusted to 1780 g/L and applied to unfired floor and fired (bisque) wall tile surfaces by a doctor blade with 0.8 mm thickness and 6 cm width. The tile samples were dried at 200 °C for 10 min in a laboratory-type drier. After drying, the floor tile samples were fired in an industrial fast-firing kiln at 1190 °C for 52 min. The wall tile samples were fired in an industrial fast-firing kiln at 1120 °C for 38 min. Colorimetric values, lightness (L\*), redness (a\*), and yellowness (b\*) based on CIELab standard, were determined by a spectrophotometer (CM 600d, Konica Minolta). CIELab coordinates were compared in color with standard engobe by calculating the color difference ( $\Delta E$ ) according to [34]:

$$\Delta E = (\Delta L^2 + \Delta a^2 + \Delta b^2)^{1/2} \quad (A)$$

To measure the water absorption and shrinkage values, the engobe slurries were dried and sieved through a 500  $\mu$ m sieve. The powder was used to form rectangular tablets by a laboratory-type press with a mold size of 5x10 cm and fired in the same firing regimes. The shrinkage was calculated by measuring the dimensions of the samples before and after the firing. For the water absorption test, the samples were weighed and then kept in boiling water for 2 h; then, water absorption was calculated from the weight difference before and after the boiling. X-ray diffraction (XRD, D8 Eco, Bruker) analysis with CuK $\alpha$  radiation, scanning range (2 $\theta$ ) of 10°-70° was performed on pelleted powders. The microstructural and compositional evaluation of the engobes were characterized by using scanning electron microscopy (SEM, Quanta FEG 450, FEI) and coupled energy dispersive spectroscopy (EDS). Coefficients of thermal expansion (DIL 402 PC, Netzsch) of the pieces from the pellets were measured up to 500 °C at 10 K/min.

## RESULTS AND DISCUSSION

Table VI shows the results of colorimetric measurement from the floor tile engobe set. Composition of the sample F2 with SiO<sub>2</sub>/Al<sub>2</sub>O<sub>3</sub> ratio of 7.88 had the highest lightness (L\*) value and sample F1 with 38.4% quartz (2.4% more than F-STD) had the lowest L\* and highest redness (a\*) values amongst the set. Except for the sample F3 with a SiO<sub>2</sub>/Al<sub>2</sub>O<sub>3</sub> ratio of 7.62, the decrease in the amount of zircon caused the yellowness (b\*) value to increase. Wall tile engobe sample

color measurement results are given in Table VII. With the decrease in the amount of zircon in the wall tile engobe compositions, the L\* value decreased, while the related value increased due to the increase in the amount of alumina. L\* values of the samples W2, W3, and W4 were higher than 91, which can be considered appropriate according to the standard sample. The sample W3 formulation with a SiO<sub>2</sub>/Al<sub>2</sub>O<sub>3</sub> ratio of 6.88 had the highest L\* value. It is important to notice that all the samples had  $\Delta E$  value lower than 1.0 which can be an acceptable threshold to judge the color difference compared to the standard ones. This  $\Delta E$  limit is used by most ceramic tile manufacturers in their quality control processes [34].

Table VI - Color values of floor tile engobe surfaces.

Color value	F-STD	F1	F2	F3	F4
L*	88.00	87.64	87.84	87.78	87.74
a*	-0.35	-0.23	-0.27	-0.31	-0.26
b*	4.46	4.56	4.65	4.12	4.70
$\Delta E$	-	0.38	0.25	0.40	0.36

Table VII - Color values of wall engobe surfaces.

Color value	W-STD	W1	W2	W3	W4
L*	91.40	90.88	91.41	91.68	91.04
a*	-0.38	-0.36	-0.48	-0.40	-0.33
b*	3.35	3.00	3.66	3.76	2.99
$\Delta E$	-	0.63	0.33	0.50	0.51

The water absorption and shrinkage behavior of the developed engobes from the floor tile set can be seen in Fig. 1a. The sample with the water absorption value closest to the standard was the sample F4 with a SiO<sub>2</sub>/Al<sub>2</sub>O<sub>3</sub> ratio of 7.92. The sample F2 had a shrinkage value closest to the standard one and its SiO<sub>2</sub>/Al<sub>2</sub>O<sub>3</sub> ratio was 7.88. When all the compositions were compared, they had similar water absorption and shrinkage values and the sample with the lowest SiO<sub>2</sub>/Al<sub>2</sub>O<sub>3</sub> ratio (7.62) showed the lowest shrinkage because of the highest alumina content. Depending on the increase in the amount of alumina in the composition

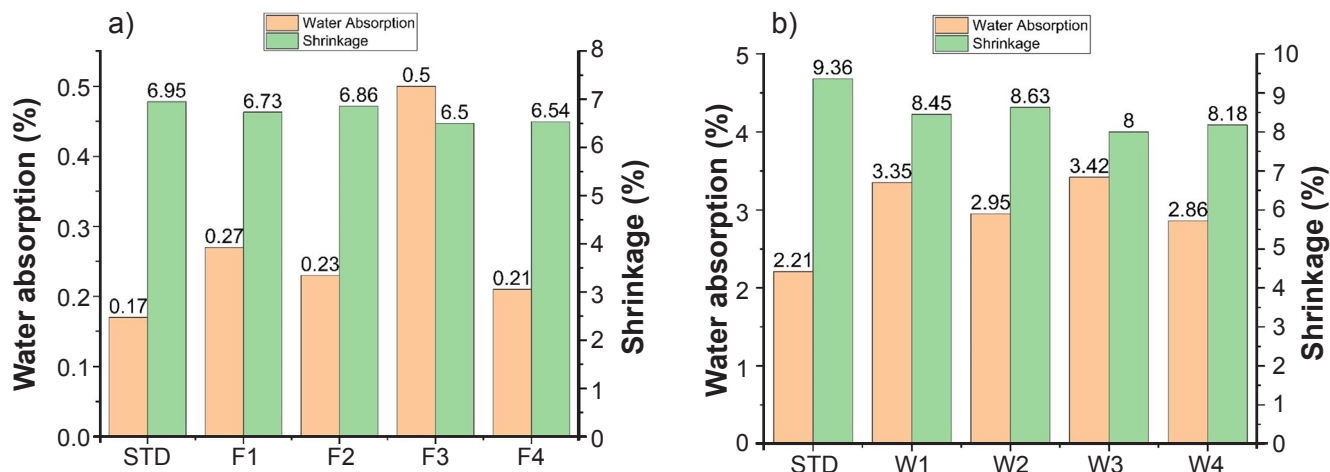


Figure 1: Shrinkage and water absorption of investigated floor (a) and wall (b) tile engobe samples.

of the engobe, the whiteness and water absorption value increased while the shrinkage value decreased since alumina influences sintering. When zircon is replaced with alumina in engobe studies, the  $L^*$  value is higher, although it becomes challenging to achieve zero water absorption at low firing temperatures [27]. All the samples except F3 showed very close results with the sample F-STD in terms of water absorption and shrinkage.

In Fig. 1b, it is clear that the water absorption of the sample W-STD which had a  $\text{SiO}_2/\text{Al}_2\text{O}_3$  ratio of 7.85 in the wall tile set was the lowest and the shrinkage amount was the highest. For sample W3 which had a minimum  $\text{SiO}_2/\text{Al}_2\text{O}_3$  ratio of 6.88, the water absorption was the highest and the shrinkage amount was the lowest among all samples. The composition with the water absorption value closest to the standard was the sample W4 and its  $\text{SiO}_2/\text{Al}_2\text{O}_3$  ratio was 7.32. The sample W2 had the shrinkage value closest to the standard and it had a  $\text{SiO}_2/\text{Al}_2\text{O}_3$  ratio of 7.25. The higher refractoriness of  $\text{Al}_2\text{O}_3$  caused a decrease in sinterability as its content increased, resulting in decreased shrinkage and increased water absorption [29]. When all the compositions were compared, the samples exhibited higher water absorption

and lower shrinkage values than the standard. Moreover, the differences in the values between the standard and the samples for the aforementioned tests were higher than the floor tile set.

Thermal expansion results of floor and wall tile engobe samples are shown in Table VIII and Table IX, respectively. From the data, changing the silica/alumina ratio and reducing the zircon amount affected the expansion behavior of engobe samples especially for floor tile formulations. Cook *et al.* [27] stated that there was no significant change in thermal expansion values when alumina was used instead of zirconia in engobe recipes. The samples F1 and W1 with the highest amount of free quartz had the highest expansion and the samples F3 and W3 with more alumina than the others in terms of  $\text{SiO}_2/\text{Al}_2\text{O}_3$  ratio had the lowest value amongst the samples. The formulations of the samples F3 and W3 presented the closest expansion values to standard ones because they had minimum quartz content contributing to balance the thermal expansion behavior of the engobe system. Another study by Bo *et al.* [35] showed that as the quantity of quartz in the engobe recipes increases, there is a higher degree of thermal expansion. For ceramic tiles to serve for many years, the thermal expansion value of the engobe should be between the glaze and body, and the expansion value of the body should be higher than the expansion value of the engobe.

XRD analysis performed on the engobe samples (Fig. 2a) showed the crystal structures present in the floor tile engobe samples. Zircon had the highest intense peak in the XRD pattern of the standard sample due to its zircon content and the peak intensity decreased gradually in the other samples. The intensity of the quartz peak in sample F1, which had the highest amount of quartz, was higher than in the other samples. It was seen some mullite peaks with low intensity in all the samples as well. As shown in Fig. 2b, there were zircon, quartz, anorthite, and titanite phases from the XRD patterns of wall tile engobe samples. It is possible the formation of titanite ( $\text{CaTiSiO}_5$ ) crystals above 1050 °C [36]. There was a visible change in the zircon and quartz peak intensities depending on the variation of all the compositions.

In Figs. 3a and 3b, a comparison between two floor tile

Table VIII - Thermal expansion coefficient ( $\alpha$ ) of floor tile engobe samples ( $10^{-7} \text{ }^\circ\text{C}^{-1}$ ).

	F-STD	F1	F2	F3	F4	Body
$\alpha$ 300 °C	61.60	65.46	64.73	62.65	64.46	66.68
$\alpha$ 400 °C	64.38	68.10	67.65	65.23	67.80	69.77
$\alpha$ 500 °C	67.32	71.75	70.50	68.87	71.15	72.15

Table IX - Thermal expansion coefficient ( $\alpha$ ) of wall tile engobe samples ( $10^{-7} \text{ }^\circ\text{C}^{-1}$ ).

	W-STD	W1	W2	W3	W4	Body
$\alpha$ 300 °C	59.57	61.22	59.52	59.33	59.85	62.15
$\alpha$ 400 °C	61.60	63.73	62.01	61.06	62.16	64.92
$\alpha$ 500 °C	63.90	66.31	64.54	63.17	64.63	67.58

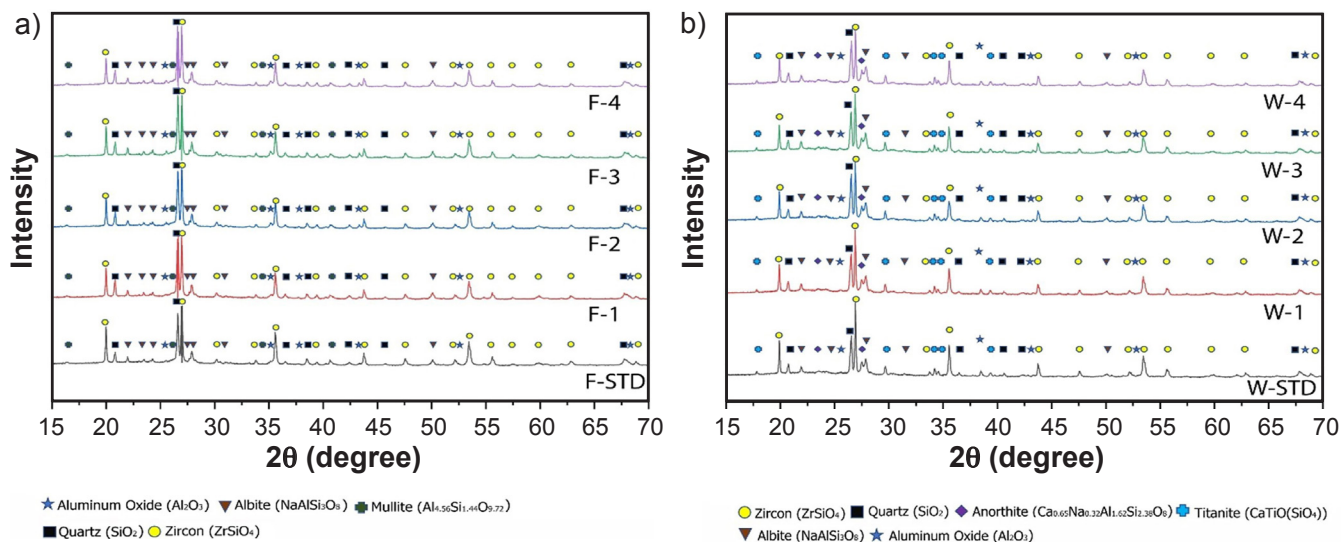


Figure 2: XRD patterns of investigated floor (a) and wall (b) tile engobe samples.

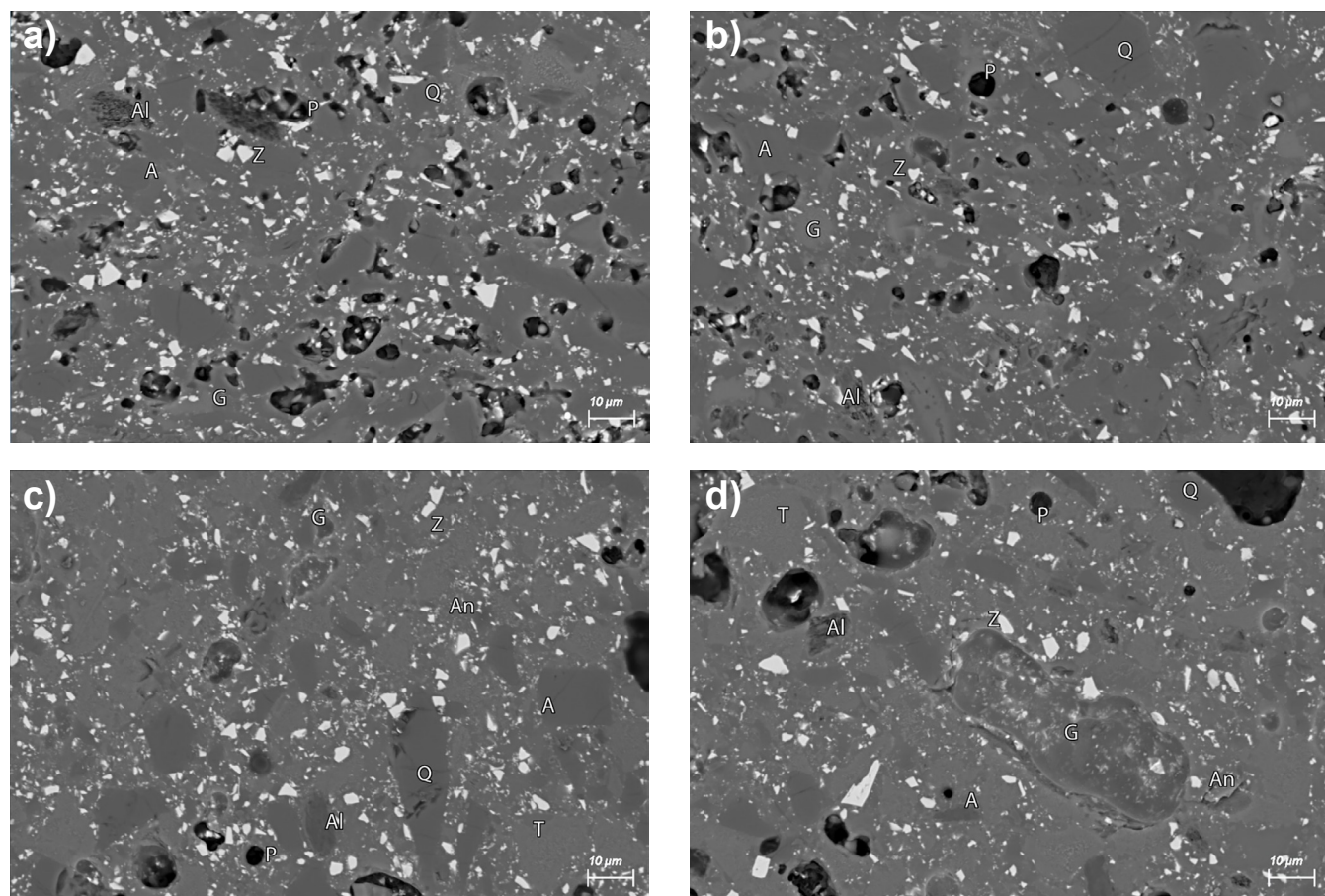


Figure 3: SEM images of engobe samples: a) F-STD; b) F2; c) W-STD; and d) W2 (A: albite, Al: alumina, An: anorthite, G: glassy phase, P: pore, Q: quartz, T: titanite, Z: zircon).

engobe microstructures can be made by SEM images, and the oxide contents determined via EDS are shown in Table X. It is possible to say that sample F2 had smaller closed pores and fewer zircon particles than the standard sample. More than 10%  $Al_2O_3$  and 25% less  $ZrO_2$  contents, which contribute to refractoriness and thermal expansion increase,

were found in the sample F2. From the images of wall tile engobe samples (Figs. 3c and 3d), sample W2 had rougher and bigger pores compared to sample F2. The increase in  $Al_2O_3$  content (Table X) may have supported the improvement of the lightness ( $L^*$ ) value of the sample W2 with less zircon content according to the standard composition.

Table X - Oxide contents (wt%) from EDS of the selected engobe samples.

Oxide	F-STD	F-2	W-STD	W-2
SiO <sub>2</sub>	59.7	58.2	62.4	58.3
Al <sub>2</sub> O <sub>3</sub>	23.2	26.0	13.2	17.0
CaO	1.0	1.2	7.0	7.2
ZrO <sub>2</sub>	8.6	7.0	6.8	6.2
Na <sub>2</sub> O	6.1	6.2	4.6	4.8
K <sub>2</sub> O	1.4	1.4	0.8	1.0
MgO	-	-	1.2	1.4
TiO <sub>2</sub>	-	-	4.0	4.1

## CONCLUSIONS

The change of SiO<sub>2</sub>/Al<sub>2</sub>O<sub>3</sub> ratio and reducing zircon (ZrSiO<sub>4</sub>) content in floor and wall tile engobe compositions were investigated. It was observed that whiteness, shrinkage, water absorption, and thermal expansion values altered with the change of SiO<sub>2</sub>/Al<sub>2</sub>O<sub>3</sub> ratio in the compositions. The zircon content varied between the engobe compositions of wall and floor tiles. The ideal engobe formulation was achieved using sample F2 which had a SiO<sub>2</sub>/Al<sub>2</sub>O<sub>3</sub> ratio of 7.88 for the floor tile surface, and sample W2 which had a SiO<sub>2</sub>/Al<sub>2</sub>O<sub>3</sub> ratio of 7.25 for the wall tile surface. The zircon content in the standard composition of the floor tile was 8 wt%. However, in the case of sample F2, the zircon content was reduced to 4.8 wt%. This engobe sample exhibited a 40% decrease in zircon content while having a SiO<sub>2</sub>/Al<sub>2</sub>O<sub>3</sub> ratio of 7.88. Additionally, the lightness (L\*) value, shrinkage, and water absorption of this sample were found to be compatible with the standard sample. Regarding the thermal expansion parameter, another sample, F3 with a SiO<sub>2</sub>/Al<sub>2</sub>O<sub>3</sub> ratio of 7.62, had the closest value to the standard sample. Based on the results obtained from the wall tile engobe set, the sample W2, which had a SiO<sub>2</sub>/Al<sub>2</sub>O<sub>3</sub> ratio of 7.25 and a zircon content of 7.2 wt%, showed values closest to the standard sample in terms of L\* and thermal expansion coefficient. The zircon content in the standard wall tile recipe, which was initially 12 wt%, was reduced by 40% to 7.2 wt% in the W2 recipe.

## REFERENCES

- [1] F. Winnefeld, *Constr. Build. Mater.* **30** (2012) 426.
- [2] M. Gajek, J. Partyka, A.R. Kmita, K. Gasek, *Ceram. Int.* **43**, 2 (2017) 1703.
- [3] M. Tarhan, *J. Therm. Anal. Calorim.* **138** (2019) 929.
- [4] F. Kara, in VII World Congr. Ceram. Tile Qual. Qualicer, Castellon (2002).
- [5] A. Barba, V. Beltran, C. Feliu, J. Garcia, F. Ginés, E. Sanchez, V. Sanz, *Materias primas para la fabricación de soportes de baldosas cerámicas*, Inst. Tecnol. Cerám., Castellón (2002).
- [6] ASTM, C373, "Standard test methods for determination of water absorption and associated properties by vacuum method for pressed ceramic tiles and glass tiles and boil method for extruded ceramic tiles and non-tile fired ceramic whiteware products", Am. Soc. Test. Mater., USA (2018).
- [7] F.B. Siqueira, *Ceram. Int.* **44**, 16 (2018) 19576.
- [8] S.O.K. Podunavac, *Acta Period. Technol.* **46** (2015) 169.
- [9] J.L. Amorós, *J. Eur. Ceram. Soc.* **30**, 1 (2010) 17.
- [10] M. Tarhan, *J. Therm. Anal. Calorim.* **140**, 2 (2020) 555.
- [11] B. Yıldız, A. Küçük, A. Kara, in XIII World Congr. Ceram. Tile Qual., Castellon (2014).
- [12] F.G. Melchiades, L.R. Santos, S. Natri, A.P. Leite, A.O. Boschi, *Interceram* **62** (2013) 16.
- [13] S. Aksan, in 6<sup>th</sup> Int. Adv. Technol. Symp., Elazığ (2011).
- [14] L.W.L. Chan, C.L. Chin, Z.A. Ahmad, S.S. Sow, in AIP Conf. Proc. **2068** (2019) 20077.
- [15] F.G. Melchiades, L.L. Silva, V.A. Silva, J.C. Romachelli, D.D.T. Vargas, A.O.E. Boschi, in Proc. VII Qualicer 2 (2002) 435.
- [16] R. Montanes, in X World Congr. Ceram. Tile Qual., Castellon (2008).
- [17] O. Khomenko, B. Datsenko, N. Siribniak, M. Nahorni, L. Tsyhanenko, *East.-Eur. J. Enterp. Technol.* **6**, 6 (2019) 49.
- [18] S. Ferrari, A. Gualtieri, *Appl. Clay Sci.* **32**, 1-2 (2006) 73.
- [19] R.A. Eppler, D.R. Eppler, *Glazes and glass coatings*, John Wiley, Ohio (2000).
- [20] R. Casasola, J.M. Rincón, M. Romero, *J. Mater. Sci.* **47**, 2 (2012) 553.
- [21] R. Pina-Zapardiel, A. Esteban-Cubillo, J.F. Bartolomé, C. Pecharromán, J.S. Moya, *J. Eur. Ceram. Soc.* **33** (2013) 3379.
- [22] E. Sanchez, M.J. Orts, J.G. Ten, V. Cantavella, *J. Am. Ceram. Soc.* **80** (2001) 43.
- [23] S. Ke, X. Cheng, Y. Wang, Q. Wang, H. Wang, *Ceram. Int.* **39**, 5 (2013) 4953.
- [24] R. Li, M. Lv, J. Cai, K. Guan, F. He, W. Li, C. Peng, P. Rao, J. Wu, *J. Eur. Ceram. Soc.* **38**, 16 (2018) 5632.
- [25] I.H. Malitson, M.J. Dodge, *J. Opt. Soc. Am.* **62** (1972) 1405.
- [26] M.K. Khan, Z.U. Rehman, S.U. Khan, in 3<sup>rd</sup> Int. Conf. Eng. Sci., Punjab (2018).
- [27] S. Cook, J. Masbate, Ch. Barrington, *Ceram. Forum Int.* **92**, 10-11 (2015) 1.
- [28] M. Leśniak, J. Partyka, K. Pasiut, M. Sitarz, *J. Mol. Struct.* **1126** (2016) 240.
- [29] S.O. Varışlı, *J. Turkish Ceram. Soc.* **1**, 4 (2022) 7.
- [30] ISO, 10545-3, "Ceramic tiles, part 3: determination of water absorption, apparent porosity, apparent relative density and bulk density", Int. Org. Stand., Geneva (2018).
- [31] ISO, 10545-8, "Ceramic tiles, part 8: determination of linear thermal expansion", Int. Org. Stand., Geneva (2018).
- [32] ISO 10545-2, "Ceramic tiles, part 2: determination of dimensions and surface quality", Int. Org. Stand., Geneva (2018).
- [33] J.L. Amorós, E. Blasco, C. Feliu, A. Moreno, *J. Non Cryst. Solids* **572** (2021) 121093.

- [34] G.M. Revel, M. Martarelli, A. Bengochea, A. Gozalbo, M.J. Orts, A. Gaki, M. Gregou, M. Taxiarchou, A. Bianchin, M. Emiliani, *Cem. Concr. Compos.* **36** (2013) 128.
- [35] M.D. Bo, A.M. Bernardin, D. Hotza, *J. Clean. Prod.* **69** (2014) 243.
- [36] L. Zhihong, Z. Mingzhen, J. Zeng, C. Peng, W. Jianqing, *Sol. Energy* **153** (2017) 623.  
(*Rec.* 20/03/2023, *Rev.* 23/06/2023, 18/08/2023, *Ac.* 05/09/2023)

